More Info at Open Access Database www.ndt.net/?id=16709

Digital Radiology with Photon Counting Detectors

Uwe ZSCHERPEL [1], David WALTER [1], Bernhard REDMER [1], Uwe EWERT [1], Christer ULLBERG [2], Niclas WEBER [2], Tuomas PANTSAR [3]

[1] Division 8.3, BAM Federal Institute for Materials Research and Testing, Berlin, Germany
Phone: +49 30 8104 3677, Fax: +49 30 8104 1837; E-mail: uwe.zscherpel@bam.de, david.walter@bam.de, bernhard.redmer@bam.de, uwe.ewert@bam.de
[2] XCounter AB, Danderyd, Sweden; E-mail: christer.ullberg@xcounter.se, niclas.weber@xcounter.se
[3] Oy Ajat Ltd, Espoo, Finland; E-mail: tuomas.pantsar@ajat.fi

Abstract
The progress in X-ray detector electronics (sensitivity and speed) allows meanwhile fast single photon detection by a matrix detector. Combined photon counting and energy discrimination is implemented in the electronic circuit of each detector pixel. The company XCounter developed detectors based on CdTe single crystals, which can be tiled to larger areas and have a pixel size of 100µm. The largest area available in beginning of 2014 is 50x75 mm². These detectors have very promising properties, which make them very suitable for NDT applications:
1. A CdTe attenuation layer of 750 µm thickness allows efficient X-ray detection up to ca. 300 keV. In counting mode only photon noise is important; no other detector noise sources need to be considered. There is no offset signal without radiation.
2. Each of the detector pixels has two energy thresholds. These can be used for dual energy imaging for materials separation. Also the suppression of scattered radiation by energy thresholding will improve the image contrast sensitivity. First experiments will be presented which demonstrate the advantages of this new detector technology over the conventional charge integrating detectors.
A challenge is the development of a modified detector calibration procedure, which becomes critical at longer exposure times.

Keywords: materials characterization, Radiographic Testing (RT), digital detector array, photo counting, image quality, calibration, dual-energy, energy discrimination

1. Introduction

Photon counting detectors offer some unique features for x-ray imaging. If designed correctly, photon counting detectors have no readout noise and no dark counts. This is an important feature for high detection efficiency and constant detector performance at various ambient temperatures requiring minimum calibration. Additionally, it is also possible to incorporate pulse height discrimination of each photon event, thus enabling the recording of images from multiple energy intervals in a single exposure. The work presented here is based on the first tests with the XCounter PDT25-DE and XC-T 7550 detectors. These detectors are based on an upgraded version of the earlier MGC700 platform [1] that now incorporates smaller pixels (100µm), dual energy thresholds and faster counting capabilities [2].

2. Detection principle and Detector construction

The Detector PDT25-DE consists of two XCounter XC225 ASICs pump-bonded to two solid-state CdTe-crystals using ohmic contacts (detection area of 25x25 mm²), whereas the XC-T 7550 detector consists of 2x6 tiles of the same modules resulting in a larger detection area of 50x75 mm². The PDT25-DE uses a USB2 interface for control and image transfer, which limits the frame rate to max. 10 frames/s. The XC-T 7550 detector implements a GBit-Ethernet interface, which allows varying the frame rate from 300 frame/s down to 2 frames/s.
Fig. 1 provides the construction principle of larger tiled detector areas. The detection crystal is bump-bonded to an underlying ASIC for pixel read-out. The ASIC XC225 has a pixel size of 100 µm and implements two counters of 12 bit each, which counts the photons passing two

adjustable thresholds (the first for discrimination of photon counting events against noise and the second for low energy counts against high energy counts).

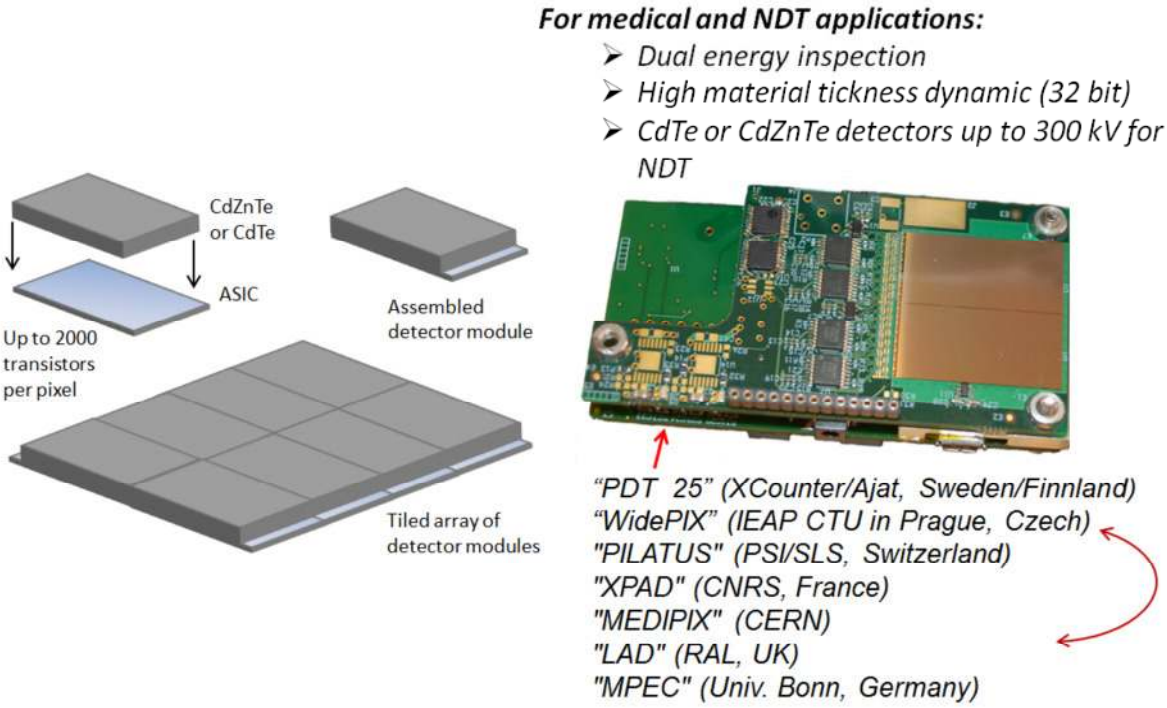

Fig. 1: State of the art of photon counting detectors in medicine and NDT (left side – construction principle of the detection area from assembled tiles, right side – image of the detector PDT-25 using 2 tiles from XCounter. Various other manufacturers exists too)

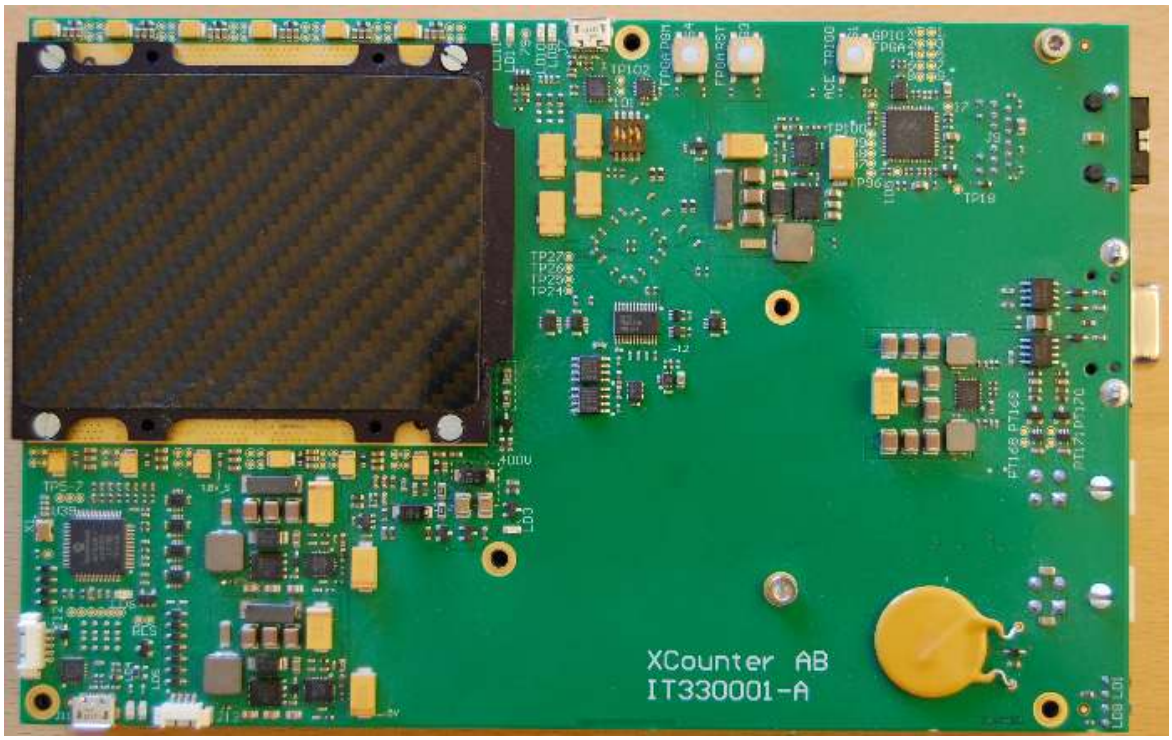

Fig. 2: View of the XC-T7550 detector with the 75x50 mm² detection area (covered by CFRP, black)

In Fig. 2 a larger detector version XC-T75550 with 75x50 mm² detector area is shown without the radiation shielding case made from Densimet. Also, the temperature stabilization of the detector ASICs using water cooled Peltier elements is not shown here.

3. Results and Discussion

3.1 Dual energy thresholding for reduced detection of scattered radiation

One major advantage of the photon counting principle is the adjustable energy threshold. Only photons having a distinct minimum threshold reaching the detector will be counted.
The usage of energy thresholding was investigated first for reduction of the influence of scattered radiation on the radiographic image. In Fig. 3 a Fe steel step wedge is shown and two images (low energy up to 80 keV and high energy image above 80 keV) as well as profiles across the steps are presented.

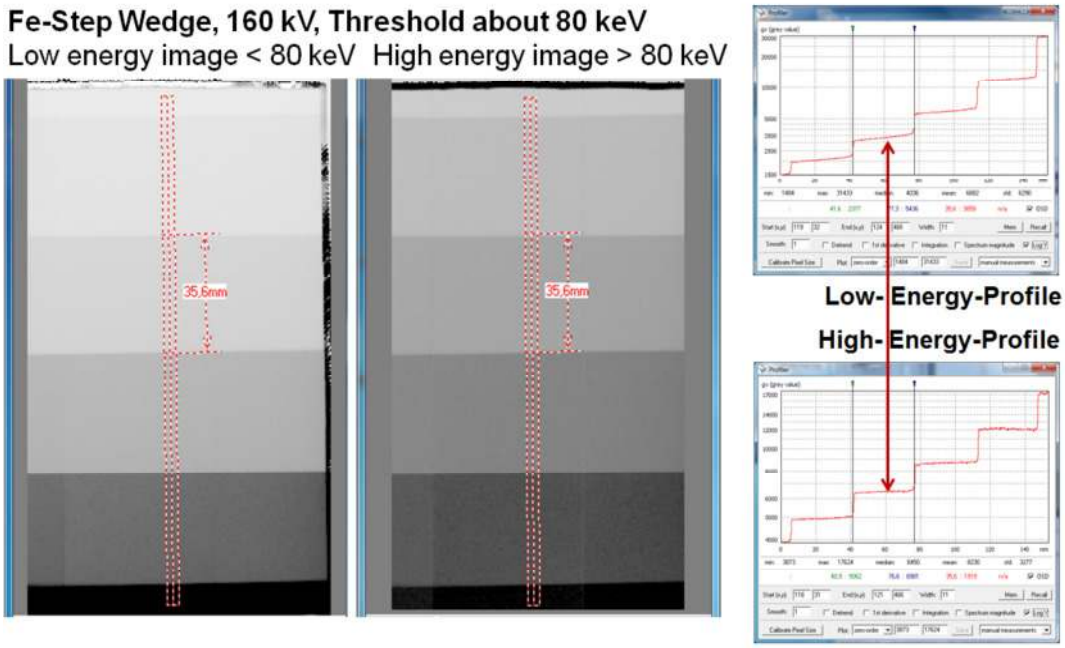

Fig. 3: Reduction of scattered radiation using the energy threshold of the photo counting detector. In the left side the low energy image and in the middle the high energy image is shown. On the right side the profiles across these images are presented. The high energy profile shows nearly no scatter artefacts as compared to the profile in the low energy image.

The profiles in Fig.3 show clearly, that the high energy image is less influenced by scattered radiation. Due to the inelastic Compton scatter effect most scattered radiation photons have lower energies than the primary photons. Scattered radiation, generated in a step wedge with homogeneous step thickness, causes in the profile a slope across each step, whereas in a step with constant thickness a constant signal is expected as derived from the attenuation law. Any changes in the profile like an increasing signal along the step with constant thickness or an overshot at the step edges appear due to contributions from scattered radiation.

3.2 Image quality measurements for high wall thicknesses of steel

The application range of this new detector generation was investigated using a double wall set-up simulating a steel pipe with 35 mm wall thickness and a source-to–detector distance of 405 mm.
In Fig 4a a schematic and in Fig. 4b a photograph of this set-up is shown. The X-ray tube parameters selected for this mobile pipe inspection were max. 270 kV and 1.11 mA.

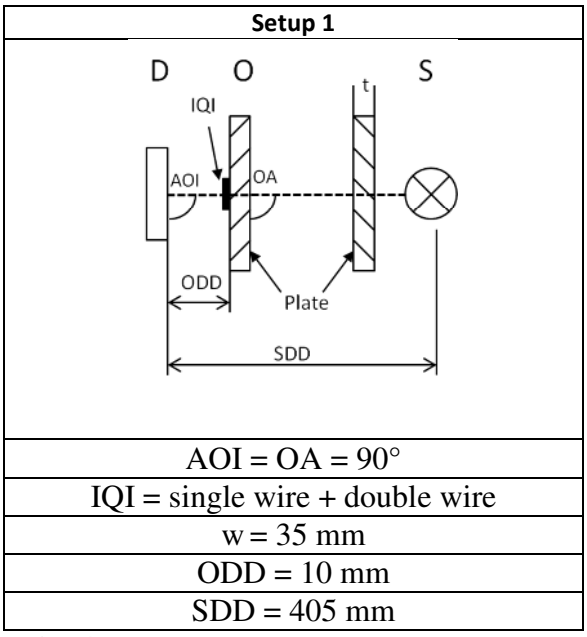

Fig. 4a: Radiography geometric setup 1

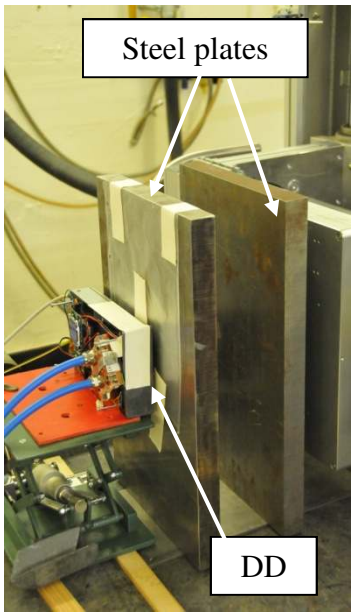

Fig. 4b: Setup 1 at BAM laboratory

For measurement of the image quality the following IQIs were used (see Fig. 5):

1. The total image unsharpness and basic spatial resolution was measured with a Duplex wire IQI according to ISO 19232-5.
2. The contrast sensitivity was measured with a single wire IQI according to ISO 19232-1

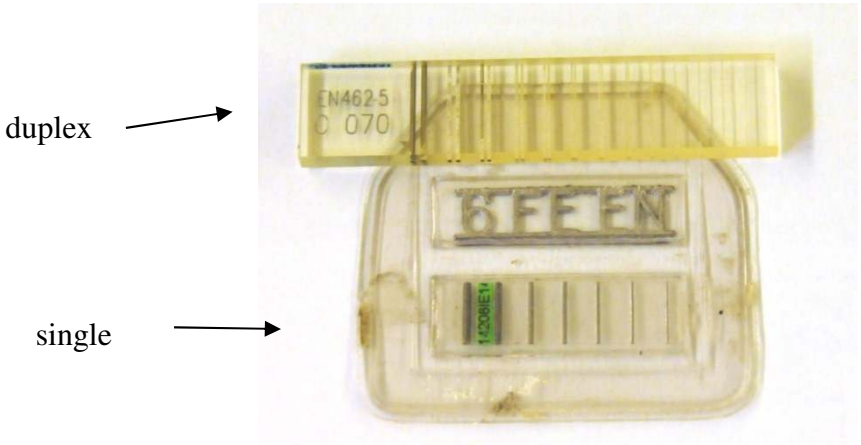

Figure 5: Duplex wire and single wire IQIs according to ISO 19232-5 and -1

One example of an acquired image with 270 kV, 1.11mA and an exposure time of 1600s is shown in Fig. 6. The Duplex wire D10 (see Fig. 7a) and single wire W11 are detected. D10 and W10 according to ISO 17636-2 are the required IQI numbers for testing class B and 35 mm nominal wall thickness, 70mm penetrated thickness, double wall penetration, single

image technique and IQIs near to the detector. These requirements of ISO 17636-2, table B.11 & B.14, are over-achieved by one single wire. There is no need to use any compensation principle. The normalized SNR in the base material is 90 (see Fig. 7b), ISO 17636-2 requires at least 70 for testing class B and w>50 mm. So, this requirement is clearly met.

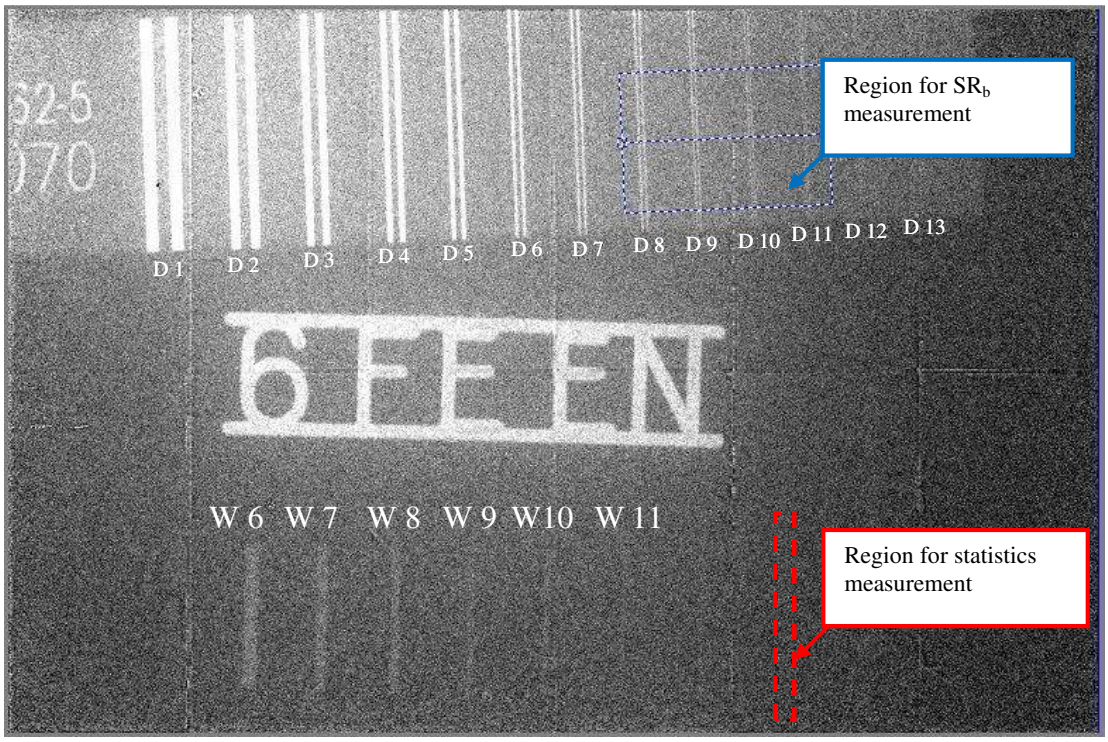

Fig. 6: Resulting image with 70 mm penetration thickness and 1600s exposure time. Single wire W11 can be detected (artefacts from tile edges are not completely suppressed)

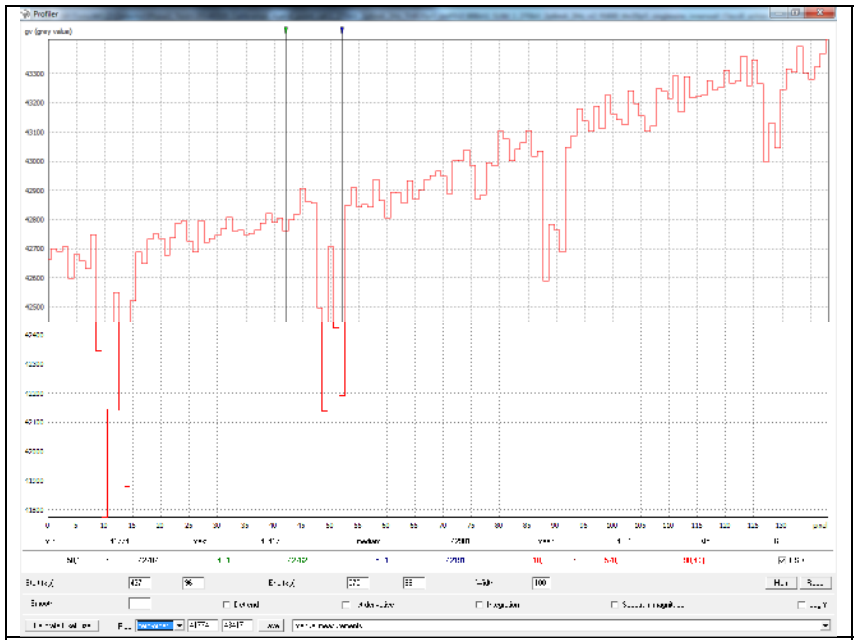

Fig. 7a: Result of SR_b measurement for 140 mm steel penetration, 90° (profile position marked in Fig. 6, D8 to D11). D 10 is not resolved with a dip >20%, the basic spatial resolution is 0.1 mm (see ISO 19232-5).

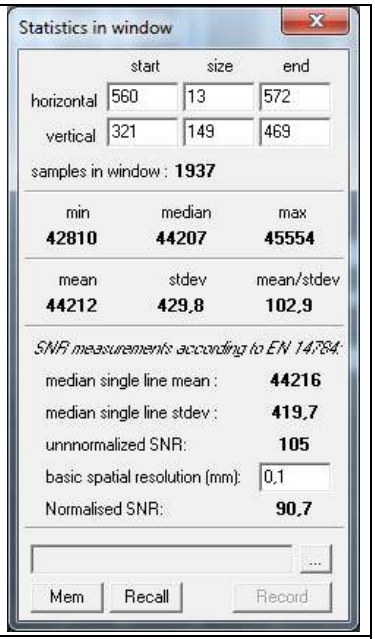

Fig. 7b: Result of statistics measurement for 70 mm steel penetration, 90° (region marked in Fig. 6)

3.3 Measurements of normalized SNR for high wall thicknesses of steel

When a detector counts the incoming photons, then the gray value Gv in the resulting image is just given by the number of detected photons per pixel. The X-ray photon flow is described by Poisson statistics, i.e. the standard deviation is just the square root of the number of photons and also of the pixel gray value. With increasing exposure the number of photons is increased and also the SNR. Caused by production tolerances of the detector, each pixel has a slightly different response, this requires a detector calibration to equalize this pixel variations. This calibration step is done using a flat field image with a homogeneous detector exposure. In [3] we developed a model for this procedure; the SNR is limited by the structure noise resulting from the limited SNR in the calibration image. A photon counting detector has a gray value efficiency Eff=1 (as defined in [3]), so the SNR model in [3] is simplified to:

$$SNR = Gv / SQRT(Gv^2/SNR^2_{max} + Gv) \qquad (1)$$

In Fig. 8 the measured normalized (by SR_b=0.1mm) SNR is given for 70mm and 100 mm wall thickness and different exposure times. Beside the measurement points several lines a given too.

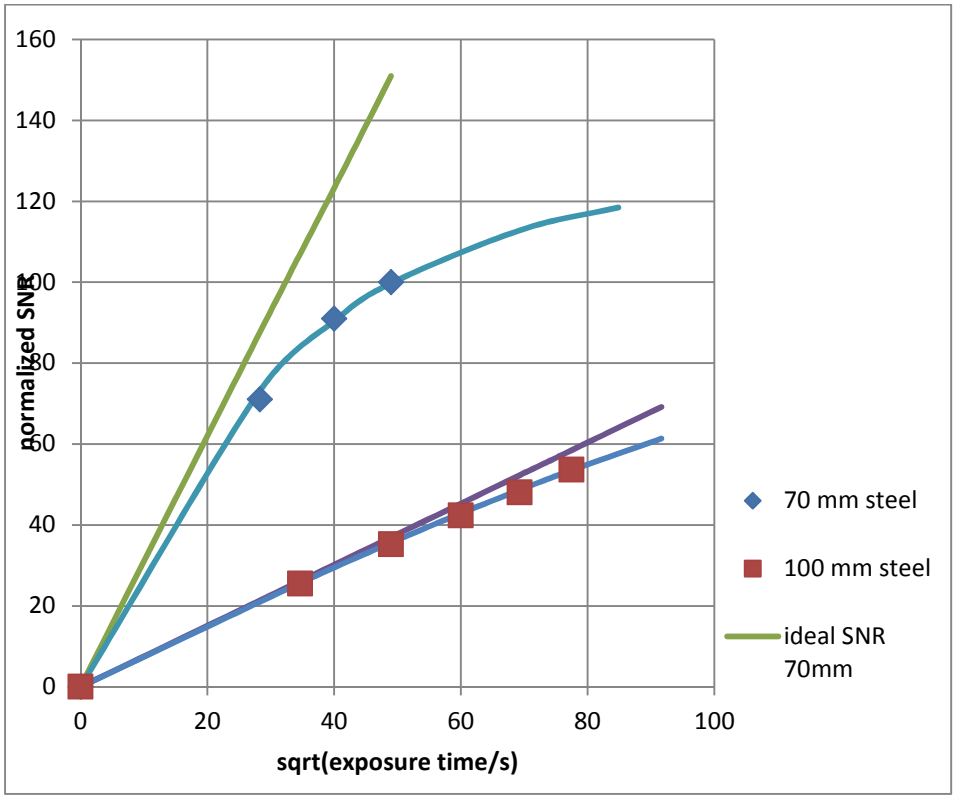

Fig.8: normalized SNR for different exposure times and 70 and 100 mm wall thickness

The lines for the ideal SNR are calculated from the square root of the gray values, which are the maximum possible SNRs for a photon counting detector. The lines "SNR fit" are the real obtained SNR curves, in both cases a SNR_{max} = 150 was used. This SNR_{max} was determined by the calibration image. The deviation for the ideal SNR line is larger for 70 mm than for 100 mm, because the gray value is for 70mm larger than for the 100 mm.
For 100 mm penetrated thickness the accumulated gray value for 1200 frames was 780, i.e. the average counting number (and gray value) in the single frame image was only 0 or 1 gray

value per frame! Even at these lowest possible gray values an image similar to that as shown in Fig 6. was detected.

3.4 Measurements of the basic spatial resolution of the detector in dependence on the angle between detector surface and the direction of incident X-ray radiation

The targeted application for this detector is the laminographic 3D reconstruction of the complete 3D volume of the pipe region under inspection, see for details [4, 5]. This is done by shifting the X-ray tube from one side of the detector to the other side. This results in varying inclination angles AOI in Fig. 4a from -45° to +45°. Results of such measurements are shown in Table 1. With a decreasing AOI the SR_b starts to decrease between 72° and 18°.
The requested SR_b according the standard EN ISO 17636-2 for class B and a penetrated thickness of 12 – 40 mm is 0.10 mm which means duplex wire D10 has to be identified. Measurements showed that class B images (regarding the SR_b) still can be achieved down to an AOI of almost 72°.
The requested SR_b according the standard EN ISO 17636-2 for class A and a wall thickness of 25 – 55 mm is 0.2 mm which means duplex wire D7 has to be identified.
The measurements summarized in Table 1 showed that even under the lowest appearing AOI of 45° (in the TomoWELD project) the SR_b is still better than the testing class A requirements and therefore acceptable.
The maximum SR_b of 0.25 mm was measured at the smallest AOI of 18° which is not mechanically achievable in the TomoWELD setup.
Despite the different penetrated thicknesses at AOI = 45° (measurements no. 5 and 6) the identified duplex wire remains the same. Only the identified single wire is reduced from W11 to W8 due to lower contrast sensitivity at equal exposure time by higher penetrated material thickness.

Table 1 Results of measurements (AOI < 90°; OA = 90°; only detector tilted)

No.	AOI	Identified duplex wire	SR_b	Identified single wire	Penetrated thickness
1	81°	D10	0.10 mm	W11	70 mm
2	72°	D10	0.10 mm	W11	70 mm
3	63°	D9	0.13 mm	W11	70 mm
4	54°	D8	0.16 mm	W11	70 mm
5	45°	D7	0.20 mm	W11	70 mm
6	45°	D7	0.20 mm	W8	100 mm
7	36°	D6	0.25 mm	W10	70 mm
8	27°	D6	0.25 mm	W9	70 mm
9	18°	D6	0.25 mm	W9	70 mm

The reason for this very good SR_b under large angles can be explained by the geometry of the setup. The thickness of the CdTe detection layer (0.75 mm) should significantly increase the measured value of SR_b. This is compensated by the reduction of the effective pixel size of the detector at 45° AOI down to 0.071 mm (1 / square root of 2), since the detector was adjusted parallel to the object surface and the duplex wire was positioned at 90° to the radiation beam, as it is required in the standard ISO 19232-5. The expected SR_b is 0.27 mm. The newly installed “anti-coincidence” function in the detector firm ware is significantly improving the

spatial resolution. When a pixel detects a signal the electronics are looking at its eight next neighbouring pixels and summing the charge from those. If the pixel has larger signals than its neighbours will count +1 and prevent the neighbours from incrementing their respective counters.

4. Conclusions

For the presented measurements the following conclusions are derived:

- The investigated photon counting detector is able to achieve testing class B for pipes with double wall single image inspection and a maximum wall thickness of 35 mm steel at 270 kV.
- The image SNR is limited by the noise in the flat field image used for detector calibration also for the photon counting detector.
- The built-in dual energy thresholding was successfully used for reduction of scattered radiation in the acquired images. This was proven by profile measurements taken from step wedge exposures.
- The basic spatial resolution of this direct converting detector is given by its pixel size.
- The basic spatial resolution is reduced to 0.20 mm at an inclination angle of 45°. This astonishing result (the detection layer has a thickness of 0.75 mm, so at 45° an SR_b of 0.27 mm is expected!) is achieved by the charge sharing correction (anti-coincidence function), which is built-in in the ASICs to reduce the spreading of charges between neighboured pixels. This compensates also for inclined X-ray radiation detection.

Aknowledgements

The work presented here has received funding from the European Union's Seventh Framework Programme for research, technological development and demonstration under grant agreement no 315213 for collaborative projects FP7-SME 2012 under "TomoWELD" (Development of Quantitative Radiographic Tomography technology for the in-situ Inspection of welded austenitic safety critical pipework in the nuclear power generation and petrochemical industries).

References

[1] K. Spartiotis, A. Leppänen et al. "A photon counting CdTe gamma and X-ray camera" Nuclear Instruments and Methods in Physics Research A 550 (2005) 267–277.

[2] C. Ullberg, M. Urech, N. Weber, A. Engman, A. Redz, F. Henckel, "Measurements of a dual-energy fast photon counting CdTe detector with integrated charge sharing correction", Proceedings of SPIE Vol. 8668, 86680P (2013) SPIE Digital Library

[3] U.Ewert, U. Zscherpel, K. Heyne, M. Jechow, K. Bavendiek, „Image Quality in Digital Industrial Radiology", Materials Evaluation, August 2012, 961- 970

[4] TomoWELD project site http://site www.tomoweld.eu

[5] U. Ewert, B. Redmer, C. Rädel, U. Schnars, R. Henrich, K. Bavendiek, and M. Jahn: Mobile Computed Tomography for Inspection of Large Stationary Components in Nuclear and Aerospace Industries, Materials Transactions 53 2 (2012), pp. 308-310.